

NASA TECHNICAL MEMORANDUM

NASA TM X- 71983

COPY NO.

NASA TM X- 71983

(NASA-TM-X-71983) TECHNIQUES FOR
AEROTHERMAL TESTS OF LARGE, FLIGHTWEIGHT
THERMAL PROTECTION PANELS IN A MACH 7
WIND TUNNEL (NASA) 10 p HC \$4.00

N74-29326

Unclas

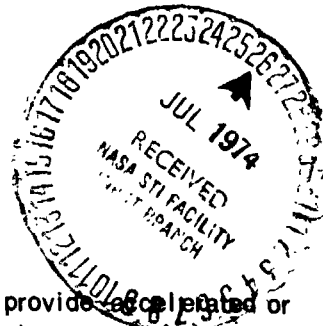
CSCL 20M G3/33

43967

TECHNIQUES FOR AEROTHERMAL TESTS OF LARGE,
FLIGHTWEIGHT THERMAL PROTECTION PANELS IN A
MACH 7 WIND TUNNEL

by

William D. Deveikis, Walter E. Bruce, Jr., and John R. Karns



This informal documentation medium is used to provide accelerated or special release of technical information to selected users. The contents may not meet NASA formal editing and publication standards, may be revised, or may be incorporated in another publication.

NATIONAL AERONAUTICS AND SPACE ADMINISTRATION
LANGLEY RESEARCH CENTER, HAMPTON, VIRGINIA 23665

TECHNIQUES FOR AEROTHERMAL TESTS OF LARGE, FLIGHTWEIGHT THERMAL PROTECTION PANELS

IN A MACH 7 WIND TUNNEL

William D. Deveikis,* Walter E. Bruce, Jr.,** and John R. Karnst
 NASA Langley Research Center
 Hampton, Virginia

Abstract

Recently developed experimental techniques permit evaluating thermal performance and structural integrity of full-scale panel concepts applicable to reentry and hypersonic vehicles in the Langley 8-foot high-temperature structures tunnel. This facility provides combinations of aerodynamic heating and pressure loading representative of flight at Mach 7 at altitudes between 25 and 40 km (80,000 and 130,000 ft) utilizing a combustion products test medium. Panels up to 108 by 152 cm (42.5 by 60 in.) are tested in two-dimensional flow at cold-wall turbulent heating rates from 29.5 to 250 kW/m² (2.6 to 22.0 Btu/ft²-sec) and at average surface pressures from 0.9 to 15.2 kPa (0.13 to 2.20 psia). Rate and magnitude of surface heating and differential-pressure loading are independently controlled. Realistic temperature distributions are radiantly preheated into the panel prior to aerodynamic heating, and stream conditions are preselected to sustain the preheat surface heating input during aerodynamic exposure. During tunnel start and shutdown, panels are shielded outside the stream from potentially damaging transient acoustics and buffeting and are then rapidly inserted into the hypersonic flow. Infrared radiometry provides detailed surveys of surface temperatures. These techniques have returned useful data from numerous tests on metal heat shields and panels with reusable surface insulation.

Introduction

Langley Research Center is conducting a test program utilizing its 8-foot high-temperature structures tunnel to provide a realistic hypersonic heating and loading environment for evaluating the thermal performance and structural integrity of the 108 by 152 cm (42.5 by 60 in.) thermal protection panels shown in Figure 1. These include metal heat shields with insulation packages and panels with nonmetallic reusable surface insulation. They were designed as full-scale hardware applicable to reentry and hypersonic vehicles and so by nature are lightweight - under 1.4 kg/m² (3 lbm/ft²) - with maximum allowable differential-pressure loading as low as 2.1 kPa (0.3 psi). To obtain meaningful experimental results, it was necessary to provide uniform two-dimensional flow over the test panel surface, to control the rate and magnitude of surface heating and of differential-pressure loading, and to avoid overstressing panels under nonrepresentative loading produced on start and shutdown periods of wind-tunnel operation. These requirements necessitated developing experimental techniques that resulted in modifying existing test

apparatus and test procedures and installing special devices. This paper reviews the test techniques and presents examples of test data to demonstrate the validity of the techniques.

Nomenclature

p	Pressure
Δp	Differential pressure
q	Heating rate
T	Temperature
t	Time
α	Angle of attack

Subscripts

t	Total condition in combustor
∞	Free stream

Test Facility

An aerial view and a schematic of the Langley 8-foot high-temperature structures tunnel are presented in Figure 2. The blowdown tunnel can simulate the aerodynamic heating and loading that is obtained in flight at a nominal Mach number of 7 in the altitude range between 25 and 40 km (80,000 and 130,000 ft). The high energy required for this simulation is obtained by burning a mixture of methane and air under pressure and expanding the resulting products of combustion to the test section Mach number through an axisymmetric contoured nozzle having an exit diameter of 2.4 m (8 ft). In the test section, the stream is a free jet with a usable test core approximately 1.2 m (4 ft) in diameter over a distance of 4.3 m (14 ft). Downstream of the test section, the flow is diffused and pumped to the atmosphere by a single-stage annular air ejector which permits low pressure, high-altitude simulation. Stagnation temperature is controlled by regulating fuel-to-air ratio to give a range of values between 1400 K and 2000 K (2500° R and 3600° R). As reported in References 1 and 2, aerodynamic pressure and heating coefficients obtained in this test medium are comparable to those obtained in test facilities using air alone. Air storage capacity provides run times up to 2 minutes.

During tunnel start and shutdown periods, models are stored in a pod below the stream to avoid the flow disturbances that are generated at those times. Once the desired flow conditions are established, a model handling system rapidly inserts a model into the stream by means of an elevator that can travel vertically over a distance of 2.13 m (7 ft) to the stream centerline in 1 second. The system can pitch models over a range of angles of attack up to $\pm 20^\circ$. Other details of this facility may be found in Reference 3.

*Aerospace Engineer, Thermal Protection Section, Structures and Dynamics Division, AIAA Member.

**Head, Structural Tunnels Section, Structures and Dynamics Division.

†Aerospace Technologist, Structural Tunnels Section, Structures and Dynamics Division.

Panel Holder

One of the most important test requirements of the present program was providing uniform pressure loading and uniform aerodynamic heating input over the test panel surface. This requirement was essentially achieved by developing the large, sting-mounted panel holder shown in Figure 3. With this fixture, surface heating and pressure loading are changed by varying angle of attack. The panel holder is a rectangular slab 141 by 300 cm (55.4 by 118 in.) with a 20° bevel at the leading edge and a cutout that can accommodate test panels up to 108 by 152 cm (42.5 by 60 in.). (In the photograph, the test panel is a metal thermal protection concept with a corrugated surface.) The panel holder is covered with a protective exterior insulation blanket of 2.54 cm (1 in.) thick Glasrock foam tiles bonded to a framework substructure of welded 2.54 cm (1 in.) thick stainless-steel members. Hinged plates on the back surface of the panel holder allow access to the underside of the test panel. A single row of spheres spaced across the panel holder width and located 13 cm (5 in.) from the sharp leading edge trips the boundary layer to provide turbulent flow over the test surface. Aerodynamic fences on the side edges of the panel holder extend 8 cm (3.0 in.) above the test surface and help channel the flow over the test panel. Inasmuch as the fence height was constrained by a test requirement for preheating the panel (to be discussed), the fences also extend 25 cm (10 in.) below the back surface of the panel holder to prevent vortical flow spilling onto the test surface from the back surface at $\alpha = 0^\circ$.

As demonstrated by the oil-flow patterns presented in Figure 4, the fences diminish the α -dependent tendency of the streamlines to deflect. The patterns were obtained on the test surface of a 1/12-scale model of the panel holder in hot flow at Mach 7. At $\alpha = 0^\circ$, the surface-pressure distribution obtained with the full-scale panel holder is uniform as shown in Figure 5. These results were obtained from tests at Mach 7 of a flat calibration panel mounted in the cutout. As indicated, virtually no vortical flow effect is present; at most, the spanwise change in pressure is about 2 percent. Pressure variations are somewhat greater at $\alpha = 10^\circ$ as shown in Figure 5(b) - ± 5 percent along the centerline and up to 12 percent spanwise near the trailing edge. Pictorial representations of turbulent heating distributions obtained from the calibration panel tests are presented in Figure 6 and show that the heating is uniform at both $\alpha = 0^\circ$ and 10° . The spanwise variation is within ± 5 percent, whereas the longitudinal heating rates characteristically decrease from the leading edge by about 15 percent. In the range of tunnel stream conditions shown in the carpet plots of Figure 7, average flat-plate surface pressures from 0.9 to 15.2 kPa (0.13 to 2.20 psia) and flat-plate, cold-wall, turbulent heating rates from 29.5 to 250 kW/m² (2.6 to 22.0 Btu/ft²-sec) are available using this panel holder. Local Mach number at the trailing edge of the calibration plate varies from about 6.5 at $\alpha = 0^\circ$ to about 4.5 at $\alpha = 15^\circ$.

Differential-Pressure Loading

Other important test requirements for performance evaluations of lightweight thermal protection panels were differential-pressure loading capability

at elevated temperatures and protection against adverse loading from rapid pressure changes on tunnel start and shutdown. (Under abnormal circumstances, the test section repressurization rate can be as high as 1 atmosphere per second.) Inasmuch as surface pressure and cold-wall heating rate are strictly a function of angle of attack under constant tunnel stream conditions, they cannot be varied independently. Nevertheless, differential pressure normal to the surface can be varied independently by controlling the cavity pressure under the panel. The differential-pressure control system consists of spring-loaded vent and fill doors, shown at the base of the panel holder in Figure 8, and a supply of nitrogen gas. The vent doors open outward and aid in evacuating the cavity during tunnel start, whereas the fill doors open inward and aid in repressurizing the cavity during tunnel shutdown. In the tunnel stream, panel loading can be varied over a range of positive (pushing the panel in) and negative (pushing the panel out) values. By venting the cavity to panel holder base pressure, the maximum α -dependent positive values of differential pressure are obtained, as shown in Figure 9. For a given α , this loading can be decreased by pressurizing the cavity with nitrogen gas. The flow of nitrogen is manually controlled. When the cavity is pressurized, the vent doors are locked using pneumatically actuated pins which automatically unlock at a preset value of differential pressure to prevent overloading the test panel.

Radiant Preheaters

For this test program, a pair of retractable banks of quartz-lamp radiant heaters was installed in the test-chamber pod for use in preheating a test panel along a programmed thermal trajectory representative of a flight heat pulse prior to inserting it into the tunnel test stream. In this manner, desired temperature distributions are obtained through the test panel that are precluded by the relatively short aerodynamic exposure times and the available heating rates. Preheating also protects against thermal overstrain that might follow the sudden exposure of a cold test panel to the hot stream. Each bank of heaters consists of 10 gold-plated, water-cooled reflector units arranged as illustrated in Figure 10. Each unit contains 16 tungsten-filament quartz lamps rated at 2000 watts. Two banks of heaters are divided into three electrical power zones. Each zone is operated by an ignitron power supply controlled by a programmed closed-loop system that follows a predetermined surface temperature trajectory. The ignitrons operate on three-phase electrical power. Their maximum output to the heaters is 1000 kilowatts. Uniformity of skin temperatures produced by the radiant heaters is within ± 34 K ($\pm 63^\circ$ R) at 1089 K (1960° R).

A steel framework carriage mounted on rails transports the heater banks by means of hydraulic motors. Full travel time in each direction is 1 second. In the extended position, the heaters cover the area of the test panel surface. Space limitations in the test-chamber pod allow a lamp height above the panel holder test surface of only 10.2 cm (4 in.).

Acoustic and Buffet Protection

Recent experience indicates that delicate, lightweight models cannot endure the airborne

acoustic disturbances associated with the subsonic-flow portion of tunnel operation and the severe buffeting during abnormal start and shutdown events. The severity of this problem is demonstrated in Figure 11 which shows a riveted corrugated Rene 41 thermal protection panel that was destroyed during an abnormally rapid shutdown. (The panel was designed for an ultimate differential-pressure loading of 21 kPa (3 psi).) Consequently, for protection against such disturbances, a pair of acoustic baffles was attached to the carriage of the retractable radiant heaters to cover the panel holder test surface and radiant heaters during tunnel start and shutdown. As illustrated in Figure 12, the baffles are trapezoidally shaped enclosures made of an aluminum plate covered on the outside with layers of felt and on the inside with sprayed-on acoustic foam. The data of Figure 13 show that the baffles attenuate the acoustic energy over the test surface by approximately 11 decibels over the range of tunnel start and shutdown combustor pressures between 1.4 and 4.1 MPa (200 and 600 psia). In service, these baffles perform very well and have repeatedly protected a corrugated Rene 41 panel (similar to panel shown in Fig. 11), a Haynes alloy panel, and a panel of reusable surface insulation (Fig. 1) against acoustic disturbances as well as buffeting during abnormal shutdowns.

To provide additional protection against acoustic disturbances and buffet loads, the normal tunnel operating procedure has been modified to reduce the static pressure during start and shutdown. Although the modified procedure consumes more air and hence sacrifices available aerodynamic exposure time (approximately 15 seconds), it works very well in practice. For example, the riveted Haynes alloy panel (Fig. 1) survived two normally controlled shutdowns without benefit of the acoustic baffles.

Scanning Infrared Radiometer

Infrared radiometry is employed for obtaining detailed coverage of surface temperatures and local hot-spot intensity. Thermal radiation is detected by means of a scanning radiometer located just outside the test stream at a distance above the test panel that yields a spatial resolution of the surface nominally 1.3 cm (1/2 in.) in diameter. The radiometer scans streamwise in 2.5 milliseconds and sweeps spanwise in 5 seconds to cover a 76.2-cm (30-in.) square with 150 scanlines. It uses a photovoltaic indium-antimonide liquid-nitrogen cooled detector having a response of 10 microseconds. The system operates in a wavelength band centered about 2.4 micrometers and is calibrated using a standard black body reference source to sense temperatures in the range between 650 K and 1300 K (1170° R and 2340° R). Output of the detector is recorded on high-frequency analog FM tape. The data are then digitized and computer processed. System calibration is corrected for the emittance of the test surface during data processing.

Test Procedure

The sequence of events during a typical wind-tunnel test of a panel is illustrated in Figure 14 which shows a spanwise cross-sectional view of the test chamber. A test begins by extending the acoustic baffles and radiant heaters over the panel surface (Fig. 14(a)) and energizing the heaters. The heaters then follow a programmed thermal trajectory that heats the panel surface at a prescribed

rate and soaks it at a specified temperature for times up to 28 minutes. During this time, selected thermocouple outputs are monitored on visual readouts, and when the panel substructure temperature approaches a specified value, either 310 K or 420 K (560° R or 760° R) the tunnel is started. (These substructure temperatures represent the heating that might occur in the panel early and late, respectively, in reentry.) Once the desired flow conditions are established, the procedure is to deenergize the heaters, retract the acoustic baffles and heaters, insert the panel into the stream, and simultaneously pitch it to a predetermined angle of attack that will sustain the preheat surface temperature (Fig. 14(b)). Usually, heater retraction and panel insertion occur within 5 seconds. During aerodynamic exposure, differential-pressure loading may be varied. At the end of the aerodynamic exposure, the procedure is reversed.

Effectiveness of Test Techniques

The techniques described herein have been successfully implemented to evaluate three thermal protection panel concepts to date. Two were riveted metal (Rene 41 and Haynes alloy 25) panels with insulation packages and one utilized bonded tiles of reusable surface insulation (LI 1500). Each panel was subjected to a prescribed number of radiant preheats and aerodynamic exposures. In all cases, it was repeatedly demonstrated that flight-weight panels can be safely isolated from the adverse acoustics and transient loading associated with startup and shutdown of this test facility. Moreover, as will be shown, the techniques allow exposure to desired, controlled test conditions.

The effectiveness of the techniques is demonstrated in Figures 15 through 18 which show data obtained during a radiant preheat/aerodynamic heating test of the corrugated Rene 41 panel (Figs. 1 and 3). As illustrated by the insert in Figure 15(a), the corrugated skin was riveted to support members 10.2 cm (4 in.) long which, in turn, were fastened to hat-section substructure members. Skin and support members were 0.05 cm (0.020 in.) thick. A 5-cm (2-in.) thick insulation package of microquartz layers rested on the substructure. The data of Figure 15 are measured temperatures from thermocouples on the skin and on a support member. The programmed thermal trajectory radiantly preheated the panel skin at a rate of 2.8 K/sec (5° R/sec) to 1089 K (1960° R) and soaked it until the substructure temperature reached 310 K (560° R). The panel was then inserted into the tunnel stream. As indicated by the thermocouple response on the skin, which was obtained near the center of the panel, the control of preheat input by the radiant heaters was very good.

For the aerodynamic heating part of this test, the panel was in the stream for 1 minute. Stagnation pressure and temperature were approximately $P_t = 17.2$ MPa (2500 psia) and $T_t = 1890$ K (3400° R). From the carpet plot of Figure 7(b), the angle of attack required for sustaining the preheat skin temperature at these conditions is approximately 9°. As shown by the thermocouple data from the wind-tunnel test in Figure 15(b), the skin temperature recovered the preheat value after a 5-second interruption of heat input prior to insertion into the stream. Thus, the preselected angle of attack was correct. The sudden drop in support-member temperatures shown on tunnel startup resulted

REPRODUCIBILITY OF THE ORIGINAL PAGE IS POOR

from aspiration during test-chamber evacuation, whereas the temperature rise rates shown after insertion resulted from the inflow of hot gases. In the tunnel stream, the uniformity of skin temperatures was within ± 28 K ($\pm 50^\circ$ R).

Corresponding panel surface pressure and differential-pressure loading data obtained are presented in Figure 16. The measured surface pressure of 8.3 kPa (1.2 psia) (Fig. 16(a)) agrees with the value extrapolated from the carpet plot of Figure 7(a) for the actual stagnation pressure of 18.2 MPa (2635 psia). For this test, the vent doors at the base of the panel holder were open to apply maximum positive differential pressure which was approximately 5 kPa (0.7 psia) at the angle of attack of 9° . Note that the differential-pressure control system maintains an unloaded panel during the rapid evacuation of the test chamber indicated by the surface-pressure response during tunnel startup.

In Figure 17, the capability of the differential-pressure control system to diminish aerodynamic loads by pressurizing the cavity is demonstrated. During this test, surface loading was increased by varying angle of attack in steps from 9° to 12° . For each increase in α , additional nitrogen was required to maintain the no-load condition. As indicated, differential pressure was maintained within ± 1.4 kPa (± 0.2 psi) once Δp -control was established.

Scanlines of surface temperatures obtained by infrared radiometry near the panel centerline are presented in Figure 18. The locations of support members and flush and round-head rivets are indicated. The area scanned by the radiometer is illustrated in the inset. The lower trace shows the heat-sink effect of support members when the panel is inserted cold, whereas the upper trace shows the stagnation-heating effect of protruding round-head rivets under near equilibrium heating conditions. Variations in surface emittance and signal noise produce apparent temperature variations along the scanlines between rivets. Agreement between infrared and thermocouple data is within 28 K (50° R). Thus, infrared radiometry is a useful tool in this test facility for providing detailed heating information that cannot readily be obtained by thermocouples.

Conclusions

Techniques have been developed for evaluating the thermal performance and structural integrity of large full-scale, lightweight thermal protection panel concepts in the Langley 8-foot high-temperature structures tunnel. The blowdown facility utilizes a high-pressure combustion process to provide an aerodynamic heating and pressure loading environment that simulates flight at a nominal Mach number of 7

in the altitude range between 25 and 40 km (80,000 and 130,000 ft). The special provisions for conducting the tests include:

1. A sting-mounted panel holder that accommodates panels up to 108 by 152 cm (42.5 by 60 in.) and provides uniform, two-dimensional turbulent flow at cold-wall heating rates from 29.5 to 250 kW/m² (2.6 to 22.0 Btu/ft²sec) and average surface pressures from 0.9 to 15.2 kPa (0.13 to 2.20 psia) by varying angle of attack.

2. A differential-pressure control system for varying panel loading and for protecting panels from adverse loading during start and shutdown periods of facility operation.

3. Acoustic baffles that shield the panel surface against adverse airborne acoustics and buffeting during the start and shutdown periods of tunnel operation and operating procedures that also attenuate noise and buffet loads in the critical range of tunnel pressures.

4. A radiant preheating system for obtaining realistic temperature distributions through the panel prior to aerodynamic exposure and for protection against overstrain resulting from the thermal shock of suddenly exposing a cold panel to aerodynamic heating; heaters are controlled to follow a programmed thermal trajectory and are coordinated with facility operations for minimal interruption of surface heating input.

5. Infrared radiometry for detailed coverage of surface heating.

These techniques have been tried and proven repeatedly. Their implementation has shown that lightweight thermal protection panel concepts, both metallic and nonmetallic, can be isolated from potentially damaging transient acoustic and pressure loading associated with tunnel start and shutdown. Furthermore, the techniques allow exposing panels to desired, controlled test conditions.

References

1. Weinstein, Irving, "Heat Transfer and Pressure Distributions on Hemisphere-Cylinders in Methane-Air Combustion Products at Mach 7," TN D-7104, 1973, NASA.
2. Howell, R. R., and Hunt, L. R., "Methane-Air Combustion Gases as an Aerodynamic Test Medium," Journal of Spacecraft and Rockets, Vol. 9, No. 1, January 1972, pp. 7-12.
3. Deveikis, William D., and Hunt, L. Roane, "Loading and Heating of a Large Flat Plate at Mach 7 in the Langley 8-Foot High-Temperature Structures Tunnel," TN D-7275, 1973, NASA.

REPRODUCIBILITY OF THE ORIGINAL PAGE IS POOR.

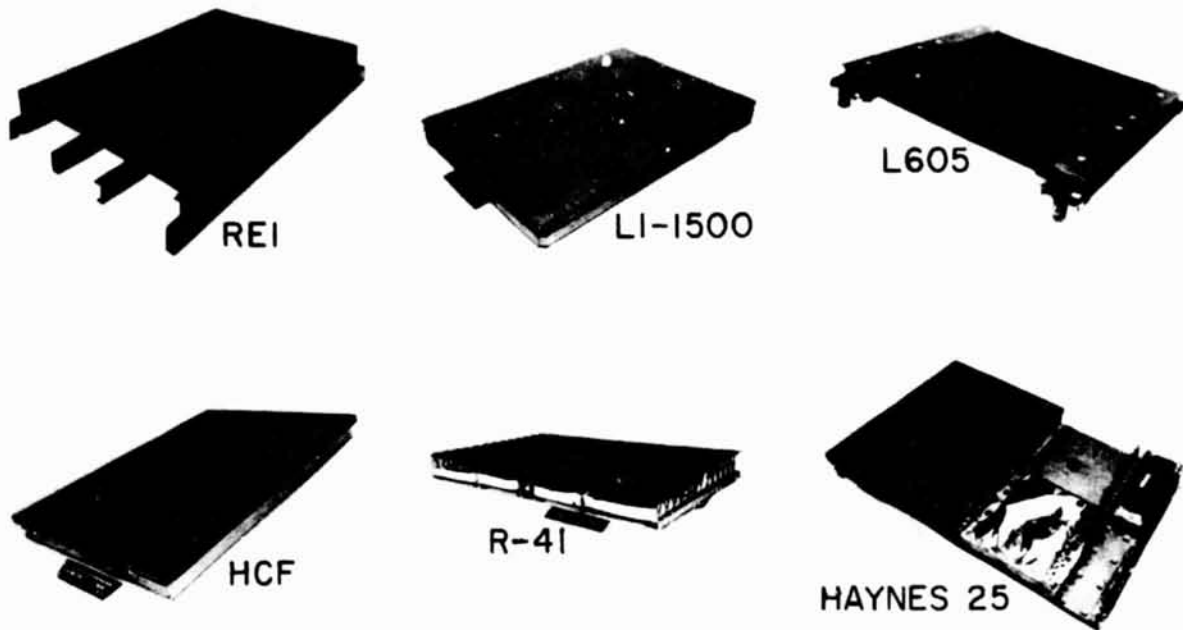
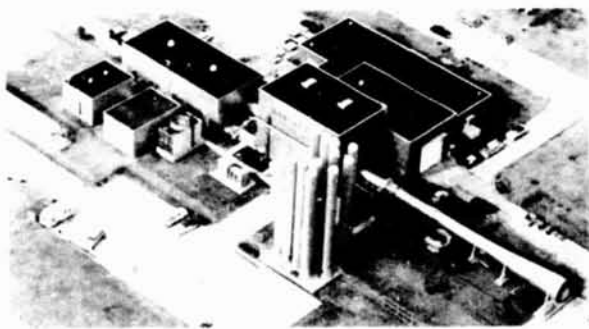
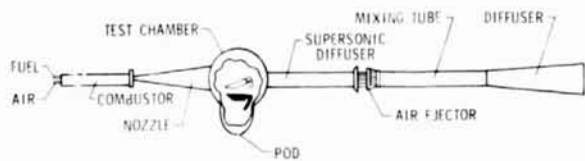


Figure 1. Typical thermal protection panel concepts.



(a) Aerial view.



(b) Schematic.

Figure 2. Views of the Langley 8-Foot High-Temperature Structures Tunnel.

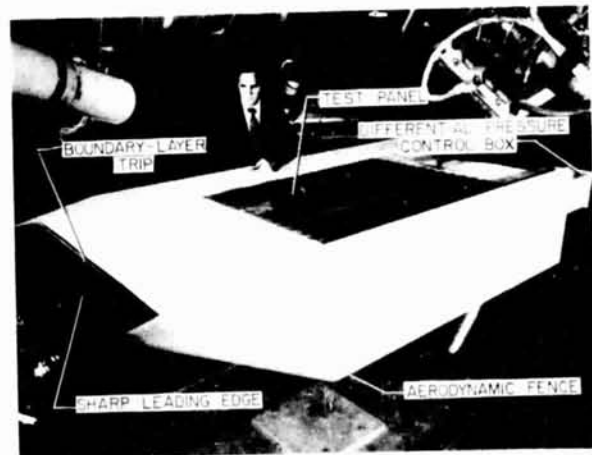


Figure 3. Panel holder with corrugated metal thermal protection panel.

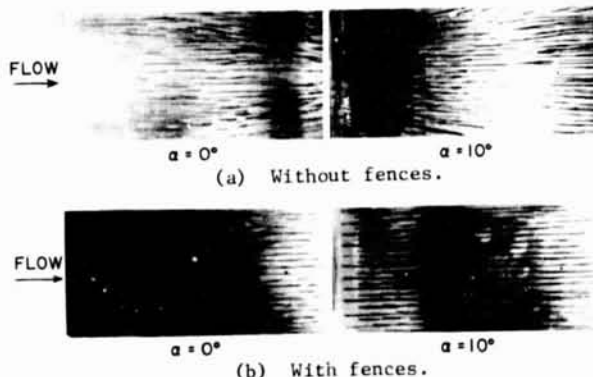


Figure 4. Oil-flow patterns on panel holder test surface.

REPRODUCIBILITY OF THE ORIGINAL PAGE IS POOR.

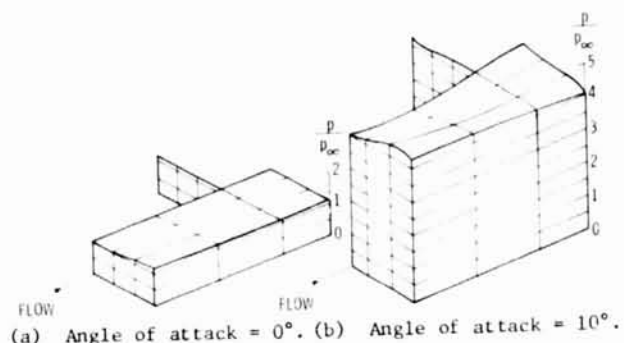


Figure 5. Pressure distributions on a flat panel mounted in the panel holder.

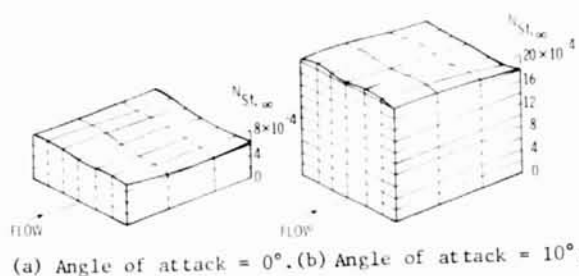


Figure 6. Heat-transfer distributions on a flat panel mounted in the panel holder.

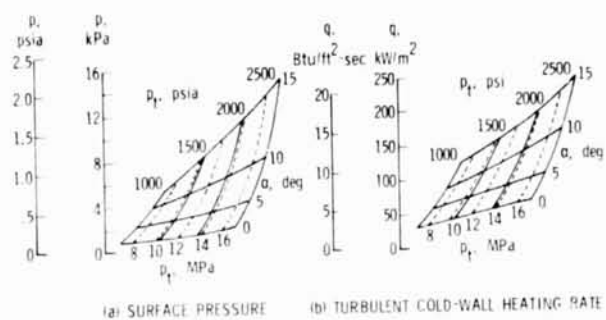


Figure 7. Average flat-plate surface pressures and cold-wall turbulent heating rates obtained with the panel holder. Total temperature = 1900 K (3400° R).

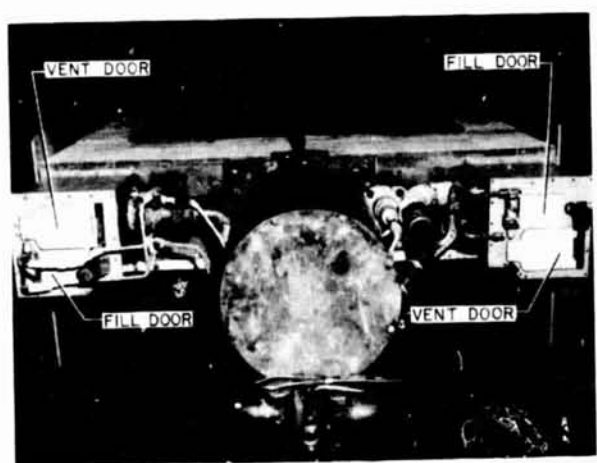


Figure 8. Differential-pressure control apparatus of panel holder.

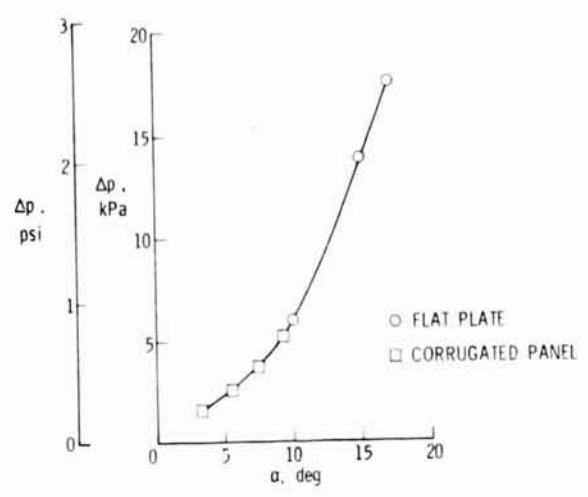


Figure 9. Maximum differential-pressure loading of test panels with angle of attack obtained by venting panel holder cavity.

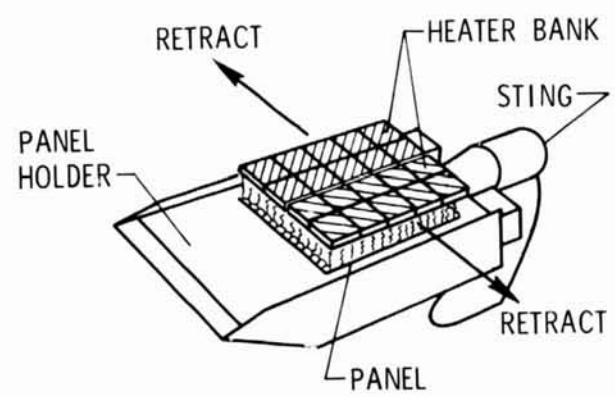


Figure 10. Sketch of retractable quartz-lamp radiant heaters extended over panel.

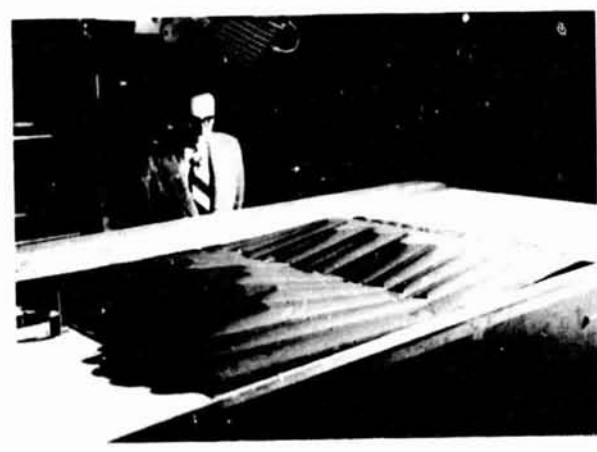


Figure 11. Photograph of test panel damaged during abnormal transient operation of Langley 8-foot high-temperature structures tunnel.

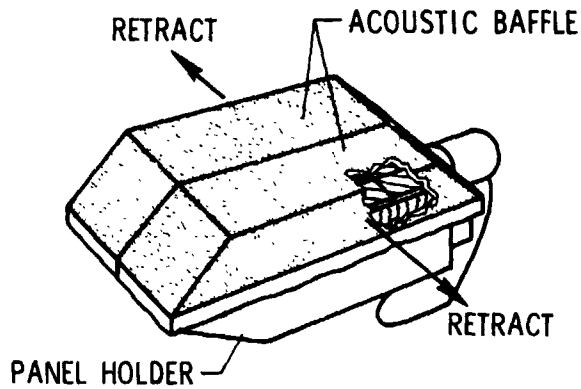
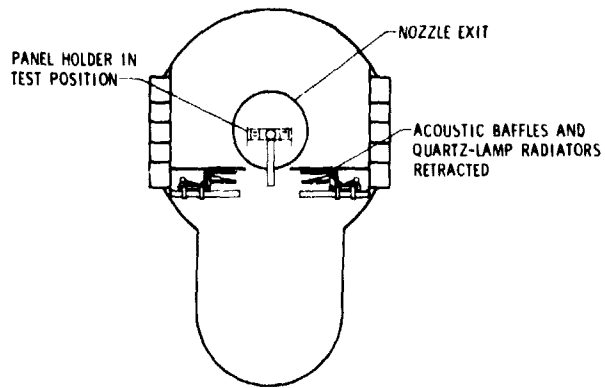


Figure 12. Sketch of retractable acoustic baffles extended over panel holder.



(b) During test.

Figure 14. Concluded.

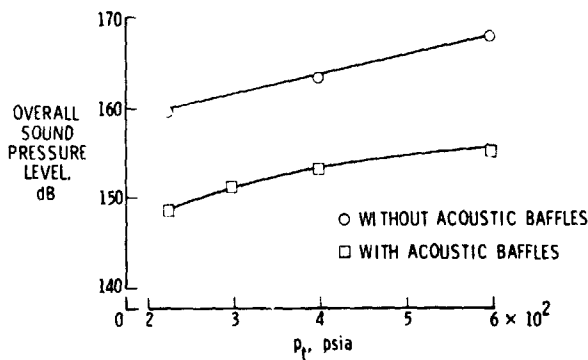
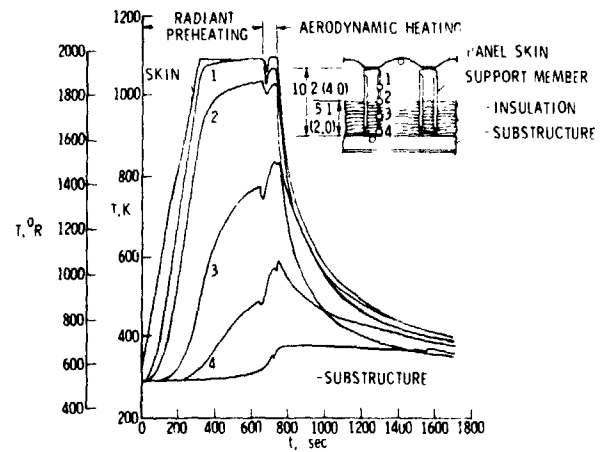
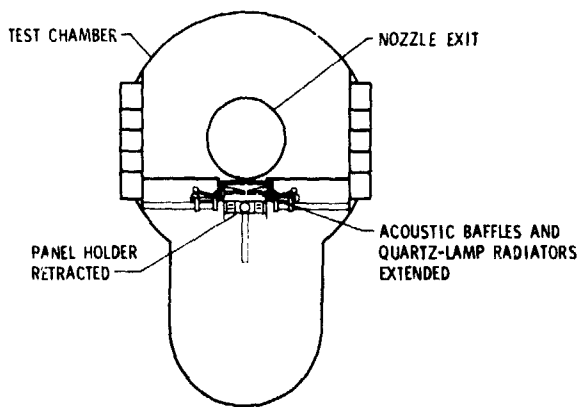


Figure 13. Effect of acoustic baffles on overall sound pressure level.

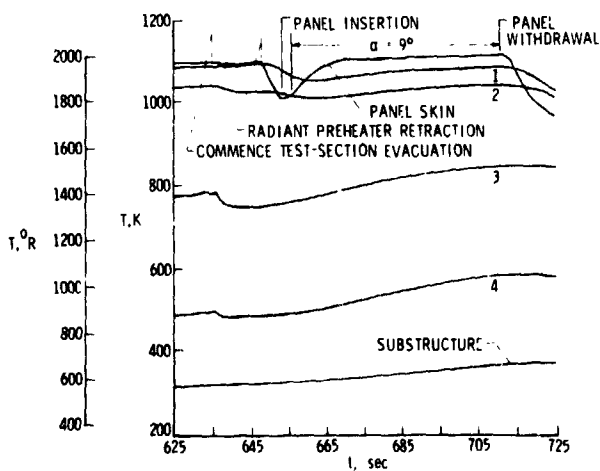


(a) Radiant preheating plus aerodynamic heating.



(a) Pretest and posttest.

Figure 14. Cross-sectional view of test section.



(b) Aerodynamic heating.

Figure 15. Thermal response of Rene 41 thermal protection panel.

REPRODUCIBILITY OF THE ORIGINAL PAGE IS POOR.

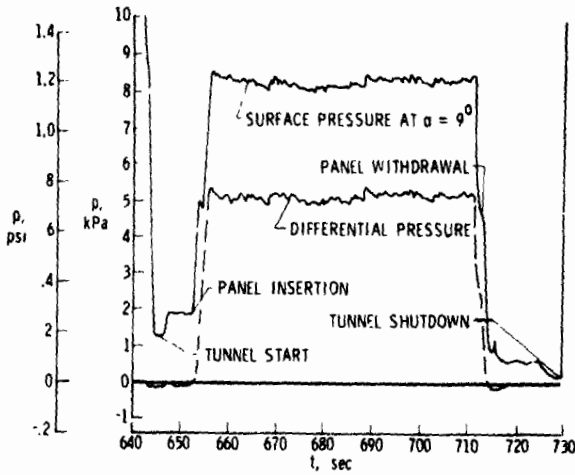


Figure 16. Panel aerodynamic loading.

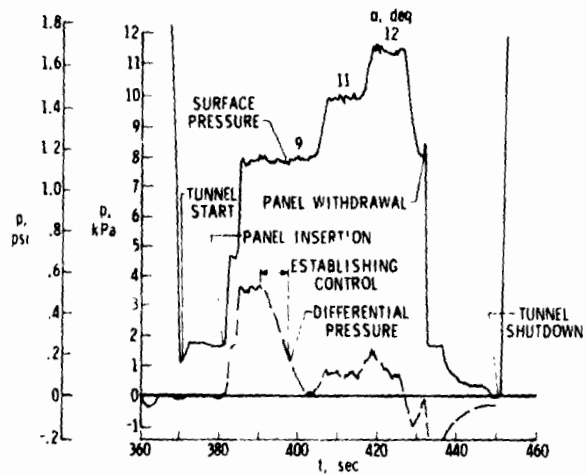


Figure 17. Capability of differential-pressure control system to reduce aerodynamic loading.

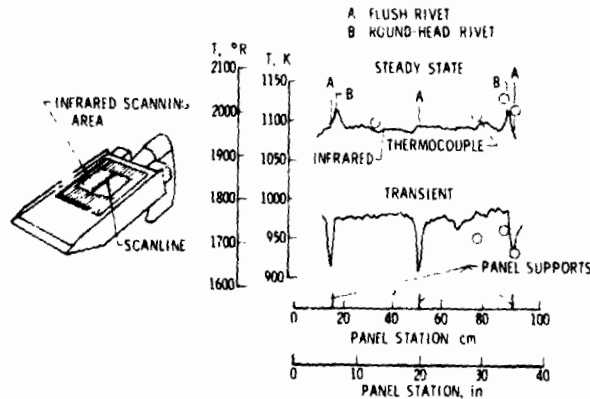


Figure 18. Surface temperatures obtained with infrared radiometry.